Published in final edited form as:
*Nat Med*. 2012 May ; 18(5): 791–798. doi:10.1038/nm.2717.

# NLRP3 has a protective role in age-related macular degeneration through the induction of IL-18 by drusen components

**Sarah L Doyle**[1,6], **Matthew Campbell**[2,6], **Ema Ozaki**[2], **Robert G Salomon**[3], **Andres Mori**[1], **Paul F Kenna**[2,4], **Gwyneth Jane Farrar**[2], **Anna-Sophia Kiang**[2], **Marian M Humphries**[2], **Ed C Lavelle**[1], **Luke A J O'Neill**[1], **Joe G Hollyfield**[5], and **Peter Humphries**[2]

[1]School of Biochemistry and Immunology, Trinity Biomedical Sciences Institute, Trinity College Dublin, Dublin 2, Ireland [2]Ocular Genetics Unit, Smurfit Institute of Genetics, Lincoln Place Gate, Trinity College Dublin, Dublin 2, Ireland [3]Department of Chemistry, Case Western Reserve University, Cleveland, Ohio, USA [4]The Research Foundation, Royal Victoria Eye and Ear Hospital, Dublin 2, Ireland [5]Department of Ophthalmology, Cole Eye Institute, Cleveland Clinic Lerner College of Medicine, Cleveland, Ohio, USA

## Abstract

Age-related macular degeneration (AMD) is the leading cause of central vision loss worldwide. Drusen accumulation is the major pathological hallmark common to both dry and wet AMD. Although activation of the immune system has been implicated in disease progression, the pathways involved are unclear. Here we show that drusen isolated from donor AMD eyes activates the NACHT, LRR and PYD domains-containing protein 3 (NLRP3) inflammasome, causing secretion of interleukin-1β (IL-1β) and IL-18. Drusen component C1Q also activates the NLRP3 inflammasome. Moreover, the oxidative-stress–related protein-modification carboxyethylpyrrole (CEP), a biomarker of AMD, primes the inflammasome. We found cleaved caspase-1 and NLRP3 in activated macrophages in the retinas of mice immunized with CEP-adducted mouse serum albumin, modeling a dry-AMD–like pathology. We show that laser-induced choroidal neovascularization (CNV), a mouse model of wet AMD, is exacerbated in *Nlrp3*$^{-/-}$ but not *Il1r1*$^{-/-}$ mice, directly implicating IL-18 in the regulation of CNV development. These findings indicate a protective role for NLRP3 and IL-18 in the progression of AMD.

In the developed world, AMD is the most prevalent cause of legal blindness in older individuals[1,2]. AMD is a progressive disease characterized by the accumulation of focal extracellular deposits on the Bruch's membrane below the retinal pigment epithelium (RPE) in the macula, which is recognized in an eye examination as drusen. The presence of drusen in the macula, the density of the deposits and the area covered by this material are used to define the early stages in the AMD disease process. Individuals with drusen are considered



Correspondence should be addressed to M.C. (matthew.campbell@tcd.ie).
[6]These authors contributed equally to this work.

Note: Supplementary information is available on the Nature Medicine website.

**AUTHOR CONTRIBUTIONS**

S.L.D. and M.C. conceived of, designed and performed experiments and wrote the paper. E.O. performed experiments. R.G.S. prepared the CEP-HSA. A.M. genotyped all animals reported in the paper and isolated cells. P.F.K. performed ERG analyses. G.J.F., A.-S.K. and M.M.H. contributed to analysis of experiments and data. E.C.L. and L.A.J.O. conceived of experiments and analyzed data. J.G.H. isolated drusen and wrote the paper. P.H. conceived of and designed experiments and wrote the paper.

**COMPETING FINANCIAL INTERESTS**

The authors declare no competing financial interests.

at risk for progressing to the end-stage blinding forms of AMD[3–5]. Geographic atrophy, the end stage of the atrophic 'dry' form of AMD, culminates in vision loss after focal degeneration of the RPE below the fovea[6]. Without the RPE, the foveal cone photoreceptors degenerate, causing central retinal blindness. CNV characterizes the end stage of the exudative 'wet' form of AMD, with new blood vessels breaking through the Bruch's membrane and the RPE that then hemorrhage, causing a blood clot to form between the RPE and the foveal photoreceptors, resulting in immediate blindness[3,4].

AMD is classically multifactorial, involving both environmental and genetic factors[7]. Sequence variants associated with disease susceptibility have now been characterized in a growing number of immune-regulated genes[8–11]. Activation of complement on ocular surfaces is thought to have a major role in the early disease process and results in drusen deposition. However, the mechanisms involved in the initiation of the inflammatory responses observed in the eyes of subjects with AMD are unresolved.

Drusen deposits are particulate protein aggregates that are extracellular in nature. These characteristics typify known activators of the sterile inflammatory response that is mediated by NLRP3. NLRP3 acts as a receptor for 'danger' signals, such as ATP, uric acid crystals, amyloid-like structures and mitochondrial dysfunction[12–15]. These danger signals activate the inflammasome, which is made up of NLRP3, apoptosis-associated speck-like domain containing a caspase-recruitment domain (ASC) and pro–caspase-1, resulting in the cleavage of pro–IL-1β and pro–IL-18 into their mature proinflammatory forms. Furthermore, excessive drusen accumulation can disrupt adjacent RPE cells, which subsequently die by necrosis[16], a cellular process now known to activate the NLRP3 inflammasome[17].

Here we show that drusen isolated from AMD donor eyes can activate the NLRP3 inflammasome. Furthermore, we show that CEP, an oxidative stress–related protein modification commonly found decorating drusen proteins[18,19], can prime the inflammasome. In tandem, we show that the complement component C1Q can activate the NLRP3 inflammasome in a caspase-1–dependent and phagolysosome-dependent manner. We observed activated caspase-1 and NLRP3 in macrophages surrounding the drusen-like lesions in mice immunized with CEP-adducted mouse serum albumin (CEP-MSA), which is a model of dry AMD. We also found that NLRP3 affects disease in a mouse model of wet AMD[20,21]. In the absence of NLRP3 in this model, CNV development was exacerbated. We implicate IL-18 as a key regulator of pathological neovascularization and suggest a protective role for the NLRP3 inflammasome in the development of AMD.

## RESULTS

The RPE is a monolayer of cuboidal cells located between the outer retina and the choroid. This melanized neuroepithelium has numerous functions, including (i) the adsorption of scattered and reflected light, (ii) the formation of the outer blood-retinal barrier and (iii) the removal by phagocytosis of the effete tips of the photoreceptor outer segments[22]. Proteomic and immunohistochemical analyses of drusen have identified virtually every protein involved in the complement cascade and the proteins found in amyloid deposits, as well as a number of crystallins, which are proteins synthesized in response to stress[23,24]. Considering the recent discovery that host-derived particulate matter such as cholesterol crystals and amyloid deposits[25,26] can activate the NLRP3 inflammasome, we were interested in determining whether drusen could also initiate the activation of the inflammasome.

### Drusen activates the NLRP3 inflammasome

We first used fundus photography to compare an unaffected eye to the eyes of individuals with either dry or wet AMD (Fig. 1a). We found punctate light deposits in the fundus

images of the eyes with wet and dry AMD, representing drusen accumulation, and we found subretinal CNV in the image of the eye with wet AMD. We sonicated the isolated drusen to dissociate the sample into small particulate matter (Fig. 1b). An SDS-PAGE analysis of the drusen sample showed a cohort of proteins of high molecular weight (greater than 60 kDa) (Fig. 1c).

The inflammasome is a multimeric protein complex. Caspase-1 is the cysteine protease that is activated in the inflammasome complex to cleave pro–IL-1β and pro–IL-18 into their mature forms. Activation of caspase-1 requires the protein ASC, which forms oligomers to create a platform for the multimeric complex. Normally, ASC is evenly distributed throughout the cell, but once activated, ASC aggregates to a single point known as a 'speck'. We primed bone-marrow–derived macrophages (BMDMs) that stably express yellow fluorescent protein–labeled ASC (YFP-ASC) with lipopolysaccharides (LPSs) and treated them with drusen or transfected them with poly(dA-dT) (positive control). ASC-YFP was difficult to discern in macrophages treated with LPS alone (Fig. 1d), however, in LPS-primed macrophages activated with drusen, the formation of intense single fluorescent specks was clearly evident, which is indicative of ASC oligomerization.

The inflammatory response associated with AMD has both a local and a systemic component. We initially tested the ARPE-19 cell line for the presence of NLRP3 and for the ability of the cells to produce IL-1β in response to a range of Toll-like receptor (TLR) ligands and activation with ATP. We found that although ARPE-19 cells express NLRP3, the amount of IL-1β in these cells was at the lower limit of the assay sensitivity (Supplementary Fig. 1). Because of their ability to access the retina in AMD, peripheral myeloid cells are probably the primary source of IL-1β and IL-18. We therefore hypothesized that these cells would be key cells of interest in our system. Human peripheral blood mononuclear cells (PBMCs) produced IL-1β and IL-18 in response to activation with drusen, even at very low concentrations (Fig. 1e,f). We used RPE material that was produced during the dissection of drusen from AMD eyes as a control for these experiments (Supplementary Fig. 2). An immunoblot analysis of caspase-1 expression in lysates of cells from the human monocytic cell line THP1 after treatment with drusen confirmed increased amounts of the cleaved caspase-1 subunit p10 (Fig. 1g and Supplementary Fig. 3). Together, these results show that drusen from AMD donor eyes can activate caspase-1 and the ASC inflammasome complex, which in turn results in IL-1β and IL-18 production in PBMCs.

We reasoned that NLRP3 was the probable sensor for drusen-induced inflammasome activation, as it is required for inflammasome activation by particulate matter. We isolated bone marrow from both wild-type (WT) and NLRP3-deficient (*Nlrp3*$^{-/-}$) mice and then used the bone marrow to culture BMDMs and bone-marrow–derived dendritic cells (BMDCs). WT BMDMs and BMDCs produced significantly higher amounts of IL-1β in response to drusen than *Nlrp3*$^{-/-}$ BMDMs and BMDCs (Fig. 1h,i), which were unable to promote the production of mature IL-1β in response to drusen. The amounts of IL-6 and tumor necrosis factor α (TNF-α) were unaltered by the presence of drusen, which is indicative of a specific effect of drusen on IL-1β production (Fig. 1h,i). These results show that AMD drusen are capable of activating the NLRP3 inflammasome.

## CEP-adducted human serum albumin primes the inflammasome

Up to 65% of the proteins that have been identified in drusen were found in drusen isolated from both AMD and non-diseased donors. However, oxidative protein modifications have also been observed in drusen, including CEP protein adducts. Cumulative oxidative damage contributes to aging and has long been suspected to contribute to the pathogenesis of AMD[27–29]. CEP adducts are uniquely generated from the oxidation of docosahexaenoate-containing lipids and are more abundant in the drusen and serum of subjects with AMD

compared to subjects without AMD[19]. Recently, carboxyalkylpyrroles, among them CEP, have been shown to be recognized by TLR2 on endothelial cells[30]. Given that TLR2 activation would prime cells to induce pro–IL-1β, pro–IL-18 and NLRP3, we hypothesized that CEP-adducted proteins in drusen and on the Bruch's membrane could represent a previously unidentified priming agent.

To test this hypothesis, we primed PBMCs with increasing concentrations of CEP-adducted human serum albumin (CEP-HSA) or HSA alone and activated the cells with ATP. The production of IL-1β increased with increasing concentrations of CEP-HSA, but we found no changes in the amount of IL-1β in cells primed with HSA alone (Fig. 2a). WT BMDMs primed with CEP-HSA and activated with ATP also produced IL-1β, an effect that we did not observe in *Nlrp3*$^{-/-}$ BMDMs (Fig. 2b). To ascertain whether CEP-HSA was priming the cells through TLR2 activation, we primed WT and *Tlr2*$^{-/-}$ BMDMs with HSA or CEP-HSA and activated them with ATP. ATP activation induced increases in IL-1β production in WT but not *Tlr2*$^{-/-}$ BMDMs primed with CEP-HSA. Furthermore, we found no IL-1β induction in BMDMs from either group primed with HSA before ATP activation, again confirming that it is CEP modification that confers the ability to activate TLR2 (Fig. 2c). IL-6 concentrations were equivalent in ATP-activated and ATP-unactivated WT cells treated with CEP-HSA, confirming the specificity of the response for IL-1β (Fig. 2d).

We measured IL-1β concentrations in LPS-primed WT and *Tlr2*$^{-/-}$ BMDMs activated by ATP to ensure that the *Tlr2*$^{-/-}$ BMDMs were responding optimally (Supplementary Fig. 4). To ensure our CEP-HSA was not contaminated with LPS, we isolated BMDMs from C3H/HeN and C3H/HeJ mice. C3H/HeJ mice carry a mutation in their *Tlr4* gene that renders them unresponsive to LPS[31]; the C3H/HeN mice do not have this mutation. C3H/HeJ BMDMs produced IL-1β in response to ATP when primed with CEP-HSA but not when primed with LPS (Fig. 2e), indicating that our CEP adduct was LPS free and primed the inflammasome through TLR2 ligation. We detected TNF-α in LPS-primed, but not CEP-primed, C3H/HeN BMDMs (Fig. 2f). We further examined the ability of CEP-HSA to prime the NLRP3 inflammasome by measuring ASC-YFP speck formation in CEP-HSA–treated immortalized WT BMDMs. We found focused ASC-YFP specks in BMDMs primed with CEP-HSA and activated with drusen (Fig. 2g). Drusen alone seemed to be able to cause the oligomerization of ASC (Fig. 2g), implying that alone, drusen could initiate the formation of the multiprotein platform for inflammasome activation. However, we were unable to consistently detect increases in IL-1β concentration when we treated PBMCs, WT BMDMs or WT BMDCs with drusen alone and assayed them using ELISA.

## Drusen component C1Q activates the inflammasome

Although drusen can distort and eventually damage the retina, as is seen in geographic atrophy[29], not all people presenting with drusen develop vision loss; therefore, it is conceivable that in addition to the particulate nature of drusen causing mechanical insult to the RPE, some component(s) of drusen may be involved in the activation of the inflammasome in a more specific manner. We elected to study C1Q, the primary initiating component of the classical complement pathway, which has been identified in drusen[32]. Because C1Q is an effector of the innate immune system and has the potential to be extremely damaging to host tissue, its presence in drusen is indicative of an earlier or ongoing inflammatory insult. We directly evaluated the ability of C1Q to activate the NLRP3 inflammasome. The addition of C1Q alone to WT BMDMs did not cause the production of IL-1β, however, cells that we primed with CEP-HSA before the addition of C1Q produced significant amounts of IL-1β compared with C1Q alone (Fig. 3a). Secretion of the proinflammatory cytokine TNF-α was unchanged after addition of C1Q to CEP-HSA–primed WT BMDMs (Fig. 3a), indicating that C1Q was specifically activating the

inflammasome and was not involved in the upregulation of proinflammatory cytokines in general. We found cleaved caspase-1 p10 in THP1 human monocytic cells activated with C1Q (Fig. 3b and Supplementary Fig. 5) and further established that C1Q can cause ASC oligomerization, as we found YFP-ASC specks in concentrated focal points within the cells activated with C1Q after priming with either LPS or CEP-HSA (Fig. 3c).

WT BMDCs treated with C1Q produced significantly more IL-1β than *Nlrp3*$^{-/-}$ BMDCs, which did not produce IL-1β in response to C1Q activation (Fig. 3d); the amount of TNF-α was the same in both groups of BMDCs after C1Q activation (Fig. 3d). To confirm the role of caspase-1, we added a caspase-1 inhibitor, Z-VAD, to human PBMCs before activation with C1Q. Caspase-1 inhibition decreased the production of both IL-1β and IL-18 in a dose-dependent manner (Fig. 3e). Together, these results show that C1Q can act as a danger signal that is sensed by the NLRP3 inflammasome. All C1Q isolated from human blood and found in drusen has a propensity to aggregate, which we have shown using a zeta-potential analysis of a solution of C1Q, and we believe this is a key factor in how C1Q can activate the NLRP3 inflammasome (Supplementary Fig. 6).

## C1Q inflammasome activation involves the phagolysosome

Deposits of C1Q, along with other complement factors, have been shown to be associated with amyloid structures or their components[33,34]. It is therefore probable that this characteristic of C1Q has a role in the aggregation of drusen. In addition, the function of C1Q in initiating opsonization would assist macrophages as they attempt to phagocytose these particulate drusen deposits. The mechanisms leading to NLRP3 inflammasome activation are unresolved and may depend on the stimulus. One proposed mechanism of NLRP3 activation involves the phagocytosis of particulate structures, leading to lysosomal rupture and the release of lysosomal contents[35]. Another proposed mechanism involves the production of reactive oxygen species (ROS), leading to the activation of the NLRP3 inflammasome through the ROS-sensitive thioredoxin interacting protein (TXNIP)[36].

To determine whether the induction by C1Q of ROS[37,38] was responsible for the inflammasome activation seen in this study, we treated PBMCs with the NADPH oxidase inhibitor diphenyliodonium (DPI) before C1Q activation. Inhibition of ROS by DPI had no effect on C1Q-induced IL-1β release (Supplementary Fig. 7a). Another alternative mechanism that has been proposed for inflammasome activation is lysosomal instability leading to the leakage of the lysosomal exopeptidase, cathepsin B, into the cytosol, which is then sensed by the components of the inflammasome, leading to its assembly[35]. To determine the role of the phagolysosome in the activation of the inflammasome by C1Q, we used bafilomycin A, an inhibitor that blocks the vacuolar $H^+$ ATPase system that is necessary for lysosomal acidification, and the cathepsin B inhibitor CA-074 Me. Inhibition of either vacuolar $H^+$ ATPase or cathepsin B restricted the C1Q-activated production of IL-1β and IL-18 with no effect on IL-6 production (Supplementary Fig. 7b,c). This implies that C1Q alters the phagolysosomal process to trigger NLRP3 activation.

## NLRP3 inflammasome is active in CEP-MSA–immunized mice

We sought to determine whether the inflammasome is involved in the pathology of a model of dry AMD, the CEP-MSA–immunized mouse model. This mouse develops AMD-like lesions in its retina and RPE after immunization with CEP-MSA.

We analyzed retinal sections of CEP-MSA–immunized mice for the presence of activated macrophages (indicated by F4/80 and CD68 staining), caspase-1 p10 and NLRP3. We found activated macrophages within the choroid and Bruch's membrane in the retinas of these mice (Fig. 4a,b and Supplementary Fig. 8). We also found infiltrating macrophages above

the RPE in the outer segments of the retinas (Fig. 4c). Staining of these sections showed colocalization of F4/80 with cleaved caspase-1 p10 (Fig. 4d,e) and NLRP3 (Fig. 4f,g and Supplementary Fig. 9).

### NLRP3 protects against exacerbated laser-induced CNV

A model for wet (exudative) AMD is laser-induced CNV, which is also an ideal model for sterile inflammation[39], probably because of the induction of a necrotic microenvironment within the tissue. Necrotic cells are known to trigger a sterile inflammatory response through the NLRP3 inflammasome[17]. We hypothesized that the NLRP3 inflammasome may have a key role in CNV development in response to localized tissue injury. To test our hypothesis, we administered focal laser burns to the retinas of WT, *Nlrp3*$^{-/-}$ and *Il1r1*$^{-/-}$ mice and assessed their CNV volumes. We found significantly more CNV development and subretinal hemorrhaging in *Nlrp3*$^{-/-}$ mice compared to WT and *Il1r1*$^{-/-}$ mice (Fig. 5a). Three-dimensional z-stack confocal volume rendering of the CNV confirmed a significantly greater ($P = 0.0496$) CNV volume in *Nlrp3*$^{-/-}$ mice 6 d after injury compared to WT and *Il1r*$^{-/-}$ mice (Fig. 5a). An electroretinographic (ERG) analysis confirmed that both groups of knockout mice had functional rod and cone responses before injury (Fig. 5b). We observed activated macrophage infiltration (positive F4/80 immunoreactivity) at the lesion sites in *Nlrp3*$^{-/-}$ mice (Fig. 5c), however, cleaved caspase-1 and IL-18 were only evident at the injury sites of WT mice and were notably absent at these sites in *Nlrp3*$^{-/-}$ mice (Fig. 5d and Supplementary Figs. 10 and 11). These findings describe a role for the NLRP3 inflammasome in the sterile inflammatory response observed in this mouse model of CNV and point toward IL-18 as a regulator of CNV development.

### NLRP3 confers protection against CNV through IL–18

To confirm a role for IL-18 in the NLRP3-mediated protection against exacerbated CNV development, we administered laser-induced CNV to *IL18*$^{-/-}$ mice. We found these mice to have normal retinal function (Fig. 6a), as assessed by an ERG analysis. Laser-induced disruption of the Bruch's membrane and a CNV volume quantification in *IL18*$^{-/-}$ mice 6 d after injury showed markedly increased lesions in the CNV from these mice (Fig. 6b) than in the CNV from WT mice (Fig. 6c). Intravitreally injecting IL-18–neutralizing antibodies subsequent to laser-induced CNV also resulted in significantly ($P = 0.0368$) increased CNV development in injected WT mice compared to WT mice that were not injected (Supplementary Fig. 12).

We reasoned that IL-18 might confer its protection through the regulation of vascular endothelial growth factor (VEGF) synthesis. To test this hypothesis, we treated ARPE-19 cells and a mouse brain microvascular endothelial cell line (bEnd.3) with recombinant IL-18 and then analyzed the VEGF concentrations in the growth medium. IL-18 significantly decreased the amount of VEGF secreted by both ARPE-19 and bEnd.3 cells (Fig. 6d,e). These findings implicate a role for IL-18 in the regulation of VEGF expression and could explain the exacerbated CNV in *Nlrp3*$^{-/-}$ and *IL18*$^{-/-}$ mice.

## DISCUSSION

Here we describe a series of observations that could have major implications for the prevention of AMD. Current antibody-based therapies target advanced forms of AMD by inhibiting the bioactivity of VEGF. However, direct and regular intraocular injection of these monoclonal antibodies (Lucentis and Avastin) carries the risk of retinal detachment, hemorrhage and infection[40].

We have shown that drusen isolated from AMD donor eyes can activate the NLRP3 inflammasome. AMD drusen is composed of a collection of protein deposits, many of which are adducted to CEP. Because of its particulate nature, it is possible that drusen from normal donor eyes may also induce inflammasome activation, however the concentrations of normal drusen in the retina, by definition, are lower than the concentrations of AMD drusen, and the biochemical compositions of the two types of drusen are different. These differences are probably crucial for the progression of AMD[41]. A comparison of normal and AMD drusen in relation to inflammasome activation, however, has not yet been made.

We have shown that CEP-HSA can prime the inflammasome through TLR2 activation, providing us with a naturally occurring priming agent that accumulates at focal points at high concentrations within the AMD eye. In the case of NLRP3, the danger signal is usually particulate and is extracellular in nature. C1Q, a component of drusen, has been shown to aggregate in an amyloid-like fashion[42]. We show that C1Q isolated from human blood activates the NLRP3 inflammasome in a manner that is dependent on lysosomal acidification and cathepsin B.

The sterile inflammatory response that occurs in AMD is probably a result of the focal necrosis that occurs in the RPE cells subadjacent to excessive drusen accumulation. Drusen accumulation in the Bruch's membrane is a hallmark feature and diagnostic indicator of early AMD development and is thought to be central to the pathology of the disease. Although we observed inflammasome activation in macrophages associated with AMD-like lesions in CEP-MSA–immunized mice, our observations indicate a protective role for inflammatory processes in the progression to CNV, the exudative form of AMD, and directly oppose the current dogma that is directed at the suppression of inflammatory processes in disease prevention. Indeed, it is now accepted that some amount of inflammation, so-called 'parainflammation', may be beneficial to the host[43,44]. From a clinical perspective, although inflammatory processes have long been associated with AMD pathology and disease development, we suggest that global inhibition of inflammation in the retina in the case of wet AMD would not be a sound therapy. Lending strength to our observations, the results of recent clinical trials of infliximab (Remicade, which targets tumor necrosis factor α (TNF-α)) in individuals with wet AMD[45,46] showed that in more than 50% of these subjects, their symptoms were greatly exacerbated. The NLRP3 inflammasome has also recently been shown to confer protection, through IL-18 production, against experimental colitis and colorectal cancer in mice[47,48]. Previous studies indicated that IL-18 has a key role in retinal vascular development. *Il18*$^{-/-}$ mice showed angiectasis and vascular leakage, and VEGF and basic fibroblast growth factor concentrations were also upregulated in the *Il18*$^{-/-}$ mouse retinas[49,50]. Anti-angiogenic roles for IL-18 have also been observed in post-ischemic injury[51] and in the inhibition of tumor angiogenesis[52].

Activation of the NLRP3 inflammasome by drusen suggests that a balance may exist whereby a certain focal amount of drusen is tolerated because of its ability to induce IL-18, which, in turn, may act as an anti-angiogenic effector, maintaining choroidal homeostasis in an inflammatory microenvironment. It is probable that once a critical level of drusen accumulates, its protective role is negated by the excessive damage to the surrounding tissues that it causes. Notably, we have shown that drusen-inducible inflammatory mediators are protective against CNV development and that it is the resultant NLRP3-mediated elevation of IL-18 concentrations that prevents the downstream production of VEGF. Moreover, IL-18 has been shown not to have a role in the development of experimental uveitis, a more conventional model of inflammation, which has direct implications for future forms of therapy deriving from our findings[53]. Overall, our observations directly implicate NLRP3 as a protective agent against the major disease pathology of AMD and suggest that

strategies aimed at producing or delivering IL-18 to the eye may be beneficial in preventing the progression of CNV in the context of wet AMD.

## ONLINE METHODS

### Drusen isolation

Drusen and minor amounts of Bruch's membrane were isolated as previously described[41] from six AMD donor eyes (88M, 91F, 97M, 85F, 85M and 80M) for use in these experiments. Human research was approved by the Research Committee, Eye and Ear Hospital, Dublin, and informed consent was obtained from all subjects.

### CEP-HSA production

HSA (Sigma-Aldrich, USA) was adducted with CEP as previously described[54].

### ELISA analysis

ELISA was used to quantify cytokines in the supernatants from the various experimental groups used throughout this study. IL-1β (R&D Systems), IL-18 (MBL International), IL-6 (R&D Systems), TNF-α (R&D Systems) and VEGF (R&D Systems) were analyzed throughout. All ELISAs were conducted a minimum of three times in triplicate. Inhibitors used during this study were added at the following concentrations 1 h before inflammasome activation: 1 μg/ml of caspase-1 inhibitor VI (Calbiochem), 5 μM cytochalasin D (Sigma-Aldrich, Ireland), 10 μM CA-074 Me (cathepsin B inhibitor) (Sigma-Aldrich, Ireland) and 10 μM DPI (Sigma-Aldrich, Ireland).

### Western blot analyses

Antibodies specific for caspase-1 (Santa Cruz Biotech), β-actin (Abcam), NLRP3 (Sigma-Aldrich, Ireland) and TLR-4 (Santa Cruz Biotech) were incubated on polyvinylidene fluoride (PVDF) membranes overnight at 4 °C. All antibodies were used at a dilution of 1:500 except β-actin, which was used at a dilution of 1:5,000. Membranes were washed with Tris-buffered saline and incubated with a secondary antibody to rabbit immunoglobulin G (IgG) with horseradish peroxidase conjugates (1:2,500) (Sigma-Aldrich, Ireland) or mouse IgG (1:1,000) (Sigma-Aldrich, Ireland) for 3 h at room temperature. Immune complexes were detected using enhanced chemiluminescence. All western blots were repeated a minimum of three times.

### Cell culture

Cells from the ARPE-19 line (American Type Culture Collection CRL 2302) were obtained from LGC Promochem, and THP1 cells and primary isolated human PBMCs were used for the *in vitro* inflammasome activation assays. Cells were cultured at 37 °C in 5% $CO_2$, 95% air in a 1:1 mixture of DMEM and Ham's F12 medium with 1.2 g/l sodium bicarbonate, 2.5 mM L-glutamine, 15 mM 4-(2-hydroxyethyl)-1-piperazine-ethanesulfonic acid (HEPES), 0.5 mM sodium pyruvate (Sigma-Aldrich) and 10% FCS. Primary BMDCs and BMDMs were also isolated from WT, *Nlrp3*$^{-/-}$, *Tlr2*$^{-/-}$, C3H/HeN and C3H/HeJ mice on a congenic C57BL/6 background. BMDCs and BMDMs were stained with antibodies to CD11c-APC and CD11b-PeCy7. Cells were gated on live single cells, and expression of CD11c and CD11b was assessed by flow cytometry (Supplementary Fig. 13). Mouse bEnd.3 microvascular endothelial cells were grown on fibronectin-coated (Sigma-Aldrich, Ireland) tissue culture flasks in DMEM containing glutamax and 10% FCS.

### ASC speck formation analyses

Immortalized BMDMs (Gift from E. Latz, University of Bonn) expressing YFP-labeled ASC were primed with LPS, HSA or CEP-HSA and then activated with drusen or C1Q for 3 or 6 h, respectively. Live-cell imaging of speck formation was undertaken using a temperature- and $CO_2^-$ regulated confocal laser scanning microscope (Olympus FluoView TM FV1000).

### CEP-MSA immunization

We used standard mouse immunization protocols[55]. We anesthetized mice with ketamine and xylazine in PBS (80–90 mg per kg of body weight of ketamine and 2–10 mg/ml of xylazine). We used 200 μg of CEP-MSA in complete Freund's adjuvant (CFA) or incomplete Freund's adjucant (IFA) (Difco Labs) for the initial dose and all booster doses, as described previously[18].

### Mouse models of CNV

All mouse experiments conducted during the course of this work adhered to the Association for Research in Vision and Ophthalmology (ARVO) standards, and approval from the Trinity College Dublin animal research ethics committee was obtained before commencement of the work. CNV, in which the vascular bed proliferates into the retina, mimicking neovascular AMD, was induced in mice using a green 532-nm Iridex Iris laser (532 nm, 140 mW, 100 mSec, 50 μm spot size, three spots per eye) incorporating a microscopic delivery system, as described previously[21]. This technique was used to induce CNV in *Nlrp3*$^{-/-}$, *Il1r1*$^{-/-}$, *IL18*$^{-/-}$ and WT mice, and in each experimental assay, the mice were age and gender matched. In tandem, we also directly injected, intravitreally after laser burn, neutralizing antibodies directed against IL-18 (Abcam). Mice were euthanized 6 d after the experiment, and their neural retinas were removed. The eye cups of the mice were then incubated with a Griffonia simplicifolia isolectin Alexa-568 molecule (Molecular Probes) (1:300) overnight at 4 °C, and CNVs were assessed by confocal microscopy (Supplementary Fig. 14a,b).

### Indirect immunostaining of retinal flatmounts and retinal cryosections

Indirect immunostaining was used to analyze activated macrophages and cleaved caspase-1, which were present in the neural retinas in the mouse models of AMD. Antibodies against F4/80, CD68 (Abcam) for activated macrophages, caspase-1 (P10) (Santa Cruz Biotech), NLRP3 (Santa Cruz Biotech and Abcam) and IL-18 (Abcam) were used at a dilution of 1:100 in conjunction with confocal laser scanning microscopy (Olympus FluoView TM FV1000).

### Statistical analyses

Statistical analyses were performed using two-tailed Student's *t* test, with statistical significance being considered at $P \leq 0.05$ when two individual experimental groups were being analyzed. For multiple comparisons, as was the case in the ELISA analyses, analysis of variance was used with a Tukey-Kramer post test, and significance was considered at $P \leq 0.05$.

### ERG analysis

ERG analysis was undertaken as previously described[56].

### Additional methods

Detailed methodology is described in the Supplementary Methods.

## Supplementary Material

Refer to Web version on PubMed Central for supplementary material.

## Acknowledgments

The Ocular Genetics Unit at Trinity College Dublin is supported by the American Health Assistance Foundation (AHAF), Science Foundation Ireland (SFI), The Health Research Board of Ireland (HRB), Irish Research Council for Science Engineering and Technology (IRCSET), Enterprise Ireland (EI), Telemedicine and Advanced Technology Research Center (TATRC) and Fighting Blindness Ireland (FB-Ireland). S.L.D. and L.A.J.O. are supported by the SFI Immunology Research Centre (IRC) and the SFI Strategic Research Cluster (07/SRC/B1144). Support for the laboratory of J.G.H. was provided by the US National Institutes of Health through grant EY014240, the Macular Vision Research Foundation, Research to Prevent Blindness and the Llura and Gordon Gund Foundation. Support for the laboratory of R.G.S. was provided by the US National Institutes of Health through grants GM021249 and EY016813. Support for the laboratory of E.C.L. was from SFI grant number 08/RFP/MBT1363 and SFI Strategic Research Cluster 07/SRC/B1144. We would like to thank C. Woods, C. Murray, D. Flynn and R. Robertson for animal husbandry. The authors would also like to thank the Research Foundation at the Royal Victoria Eye and Ear Hospital for assistance in the acquisition of the Iridex laser system. We thank E. Latz (University of Bonn) for the provision of BMDMs expressing YFP-labeled ASC. We would like to acknowledge the expertise of K. Shadrach in isolating drusen from AMD donor eyes.

## References

1. Swaroop A, Chew EY, Rickman CB, Abecasis GR. Unravelling a multifactorial late-onset disease: from genetic susceptibility to disease mechanisms for age-related macular degeneration. Annu. Rev. Genomics Hum. Genet. 2009; 10:19–43. [PubMed: 19405847]
2. Resnikoff S, et al. Global data on visual impairment in the year 2002. Bull. World Health Organ. 2004; 82:844–851. [PubMed: 15640920]
3. Bressler SB, Maguire MG, Bressler NM, Fine SL. Relationship of drusen and abnormalities of the retinal pigment epithelium to the prognosis of neovascular macular degeneration. The Macular Photocoagulation Study Group. Arch. Ophthalmol. 1990; 108:1442–1447. [PubMed: 1699513]
4. Sarks SH, van Driel D, Maxwell L, Killingsworth M. Softening of drusen and subretinal neovascularization. Trans. Ophthalmol. Soc. U.K. 1980; 100:414–422. [PubMed: 6171074]
5. Vinding T. Occurrence of drusen, pigmentary changes, and exudative changes in the macula with reference to age-related macular degeneration. An epidemiological study of 1000 aged individuals. Acta Ophthalmol. (Copenh.). 1990; 68:410–414. [PubMed: 2220356]
6. Holz FG, Bellman C, Staudt S, Schutt F, Volcker HE. Fundus autofluorescence and development of geographic atrophy in age-related macular degeneration. Invest. Ophthalmol. Vis. Sci. 2001; 42:1051–1056. [PubMed: 11274085]
7. Seddon JM, George S, Rosner B. Cigarette smoking, fish consumption, omega-3 fatty acid intake, and associations with age-related macular degeneration: the US Twin Study of Age-Related Macular Degeneration. Arch. Ophthalmol. 2006; 124:995–1001. [PubMed: 16832023]
8. Edwards AO, Malek G. Molecular genetics of AMD and current animal models. Angiogenesis. 2007; 10:119–132. [PubMed: 17372852]
9. Canter JA, et al. Mitochondrial DNA polymorphism A4917G is independently associated with age-related macular degeneration. PLoS ONE. 2008; 3:e2091. [PubMed: 18461138]
10. Chen Y, Bedell M, Zhang K. Age-related macular degeneration: genetic and environmental factors of disease. Mol. Interv. 2010; 10:271–281. [PubMed: 21045241]
11. Leveziel N, et al. Genetic factors associated with age-related macular degeneration. Ophthalmologica. 2011; 226:87–102. [PubMed: 21757876]
12. Mariathasan S, et al. Cryopyrin activates the inflammasome in response to toxins and ATP. Nature. 2006; 440:228–232. [PubMed: 16407890]
13. Martinon F, Pétrilli V, Mayor A, Tardivel A, Tschopp J. Gout-associated uric acid crystals activate the NALP3 inflammasome. Nature. 2006; 440:237–241. [PubMed: 16407889]
14. Halle A, et al. The NALP3 inflammasome is involved in the innate immune response to amyloid-β. Nat. Immunol. 2008; 9:857–865. [PubMed: 18604209]

15. Zhou R, Yazdi AS, Menu P, Tschopp J. A role for mitochondria in NLRP3 inflammasome activation. Nature. 2011; 469:221–225. [PubMed: 21124315]
16. Gao H, Hollyfield JG. Aging of the human retina. Differential loss of neurons and retinal pigment epithelial cells. Invest. Ophthalmol. Vis. Sci. 1992; 33:1–17. [PubMed: 1730530]
17. Iyer SS, et al. Necrotic cells trigger a sterile inflammatory response through the Nlrp3 inflammasome. Proc. Natl. Acad. Sci. USA. 2009; 106:20388–20393. [PubMed: 19918053]
18. Hollyfield JG, et al. Oxidative damage-induced inflammation initiates age-related macular degeneration. Nat. Med. 2008; 14:194–198. [PubMed: 18223656]
19. Gu X, et al. Carboxyethylpyrrole protein adducts and autoantibodies, biomarkers for age-related macular degeneration. J. Biol. Chem. 2003; 278:42027–42035. [PubMed: 12923198]
20. Sakurai E, et al. Macrophage depletion inhibits experimental choroidal neovascularization. Invest. Ophthalmol. Vis. Sci. 2003; 44:3578–3585. [PubMed: 12882810]
21. Campbell M, et al. Systemic low molecular weight drug delivery to pre-selected neuronal regions. EMBO Mol. Med. 2011; 3:235–245. [PubMed: 21374818]
22. Ma W, Zhao L, Fontainhas AM, Fariss RN, Wong WT. Microglia in the mouse retina alter the structure and function of retinal pigmented epithelial cells: a potential cellular interaction relevant to AMD. PLoS ONE. 2009; 4:e7945. [PubMed: 19936204]
23. Anderson DH, et al. Characterization of β amyloid assemblies in drusen: the deposits associated with aging and age-related macular degeneration. Exp. Eye Res. 2004; 78:243–256. [PubMed: 14729357]
24. Luibl V, et al. Drusen deposits associated with aging and age-related macular degeneration contain nonfibrillar amyloid oligomers. J. Clin. Invest. 2006; 116:378–385. [PubMed: 16453022]
25. Duewell P, et al. NLRP3 inflammasomes are required for atherogenesis and activated by cholesterol crystals. Nature. 2010; 464:1357–1361. [PubMed: 20428172]
26. Masters SL, et al. Activation of the NLRP3 inflammasome by islet amyloid polypeptide provides a mechanism for enhanced IL-1β in type 2 diabetes. Nat. Immunol. 2010; 11:897–904. [PubMed: 20835230]
27. Lin H, et al. Mitochondrial DNA damage and repair in RPE associated with aging and age-related macular degeneration. Invest. Ophthalmol. Vis. Sci. 2011; 52:3521–3529. [PubMed: 21273542]
28. Wang AL, et al. Autophagy, exosomes and drusen formation in age-related macular degeneration. Autophagy. 2009; 5:563–564. [PubMed: 19270489]
29. Zarbin MA. Current concepts in the pathogenesis of age-related macular degeneration. Arch. Ophthalmol. 2004; 122:598–614. [PubMed: 15078679]
30. West XZ, et al. Oxidative stress induces angiogenesis by activating TLR2 with novel endogenous ligands. Nature. 2010; 467:972–976. [PubMed: 20927103]
31. Poltorak A, et al. Defective LPS signaling in C3H/HeJ and C57BL/10ScCr mice: mutations in Tlr4 gene. Science. 1998; 282:2085–2088. [PubMed: 9851930]
32. Hageman GS, Mullins RF. Molecular composition of drusen as related to substructural phenotype. Mol. Vis. 1999; 5:28. [PubMed: 10562652]
33. Nauta AJ, et al. Direct binding of C1q to apoptotic cells and cell blebs induces complement activation. Eur. J. Immunol. 2002; 32:1726–1736. [PubMed: 12115656]
34. Blanquet-Grossard F, Thielens NM, Vendrely C, Jamin M, Arlaud GJ. Complement protein C1q recognizes a conformationally modified form of the prion protein. Biochemistry. 2005; 44:4349–4356. [PubMed: 15766264]
35. Hornung V, et al. Silica crystals and aluminum salts activate the NALP3 inflammasome through phagosomal destabilization. Nat. Immunol. 2008; 9:847–856. [PubMed: 18604214]
36. Zhou R, Tardivel A, Thorens B, Choi I, Tschopp J. Thioredoxin-interacting protein links oxidative stress to inflammasome activation. Nat. Immunol. 2010; 11:136–140. [PubMed: 20023662]
37. Luo X, Weber GA, Zheng J, Gendelman HE, Ikezu T. C1q-calreticulin induced oxidative neurotoxicity: relevance for the neuropathogenesis of Alzheimer's disease. J. Neuroimmunol. 2003; 135:62–71. [PubMed: 12576225]
38. Ten VS, et al. Complement component c1q mediates mitochondria-driven oxidative stress in neonatal hypoxic-ischemic brain injury. J. Neurosci. 2010; 30:2077–2087. [PubMed: 20147536]

39. McDonald B, et al. Intravascular danger signals guide neutrophils to sites of sterile inflammation. Science. 2010; 330:362–366. [PubMed: 20947763]
40. CATT Research Group. Ranibizumab and bevacizumab for neovascular age-related macular degeneration. N. Engl. J. Med. 2011; 364:1897–1908. [PubMed: 21526923]
41. Crabb JW, et al. Drusen proteome analysis: an approach to the etiology of age-related macular degeneration. Proc. Natl. Acad. Sci. USA. 2002; 99:14682–14687. [PubMed: 12391305]
42. Ishii T, Haga S, Yagishita S, Tateishi J. The presence of complements in amyloid plaques of Creutzfeldt-Jakob disease and Gerstmann-Straussler-Scheinker disease. Appl. Pathol. 1984; 2:370–379. [PubMed: 6400466]
43. Xu H, Chen M, Forrester JV. Para-inflammation in the aging retina. Prog. Retin. Eye Res. 2009; 28:348–368. [PubMed: 19560552]
44. Medzhitov R. Origin and physiological roles of inflammation. Nature. 2008; 454:428–435. [PubMed: 18650913]
45. Arias L, et al. Intravitreal infliximab in patients with macular degeneration who are nonresponders to antivascular endothelial growth factor therapy. Retina. 2010; 30:1601–1608. [PubMed: 21060271]
46. Giganti M, et al. Adverse events after intravitreal infliximab (Remicade). Retina. 2010; 30:71–80. [PubMed: 19996827]
47. Dupaul-Chicoine J, et al. Control of intestinal homeostasis, colitis, and colitis-associated colorectal cancer by the inflammatory caspases. Immunity. 2010; 32:367–378. [PubMed: 20226691]
48. Allen IC, et al. The NLRP3 inflammasome functions as a negative regulator of tumorigenesis during colitis-associated cancer. J. Exp. Med. 2010; 207:1045–1056. [PubMed: 20385749]
49. Qiao H, et al. Abnormal retinal vascular development in IL-18 knockout mice. Lab. Invest. 2004; 84:973–980. [PubMed: 15122309]
50. Qiao H, et al. Interleukin-18 regulates pathological intraocular neovascularization. J. Leukoc. Biol. 2007; 81:1012–1021. [PubMed: 17234681]
51. Mallat Z, et al. Interleukin-18/interleukin-18 binding protein signaling modulates ischemia-induced neovascularization in mice hindlimb. Circ. Res. 2002; 91:441–448. [PubMed: 12215494]
52. Coughlin CM, et al. Interleukin-12 and interleukin-18 synergistically induce murine tumor regression which involves inhibition of angiogenesis. J. Clin. Invest. 1998; 101:1441–1452. [PubMed: 9502787]
53. Jiang HR, et al. IL-18 not required for IRBP peptide-induced EAU: studies in gene-deficient mice. Invest. Ophthalmol. Vis. Sci. 2001; 42:177–182. [PubMed: 11133864]
54. Gu X, et al. Oxidatively truncated docosahexaenoate phospholipids: total synthesis, generation, and peptide adduction chemistry. J. Org. Chem. 2003; 68:3749–3761. [PubMed: 12737551]
55. Percopo CM, Hooks JJ, Shinohara T, Caspi R, Detrick B. Cytokine-mediated activation of a neuronal retinal resident cell provokes antigen presentation. J. Immunol. 1990; 145:4101–4107. [PubMed: 2147935]
56. Marmor MF, et al. ISCEV Standard for full-field clinical electroretinography (2008 update). Doc. Ophthalmol. 2009; 1:69–77. [PubMed: 19030905]

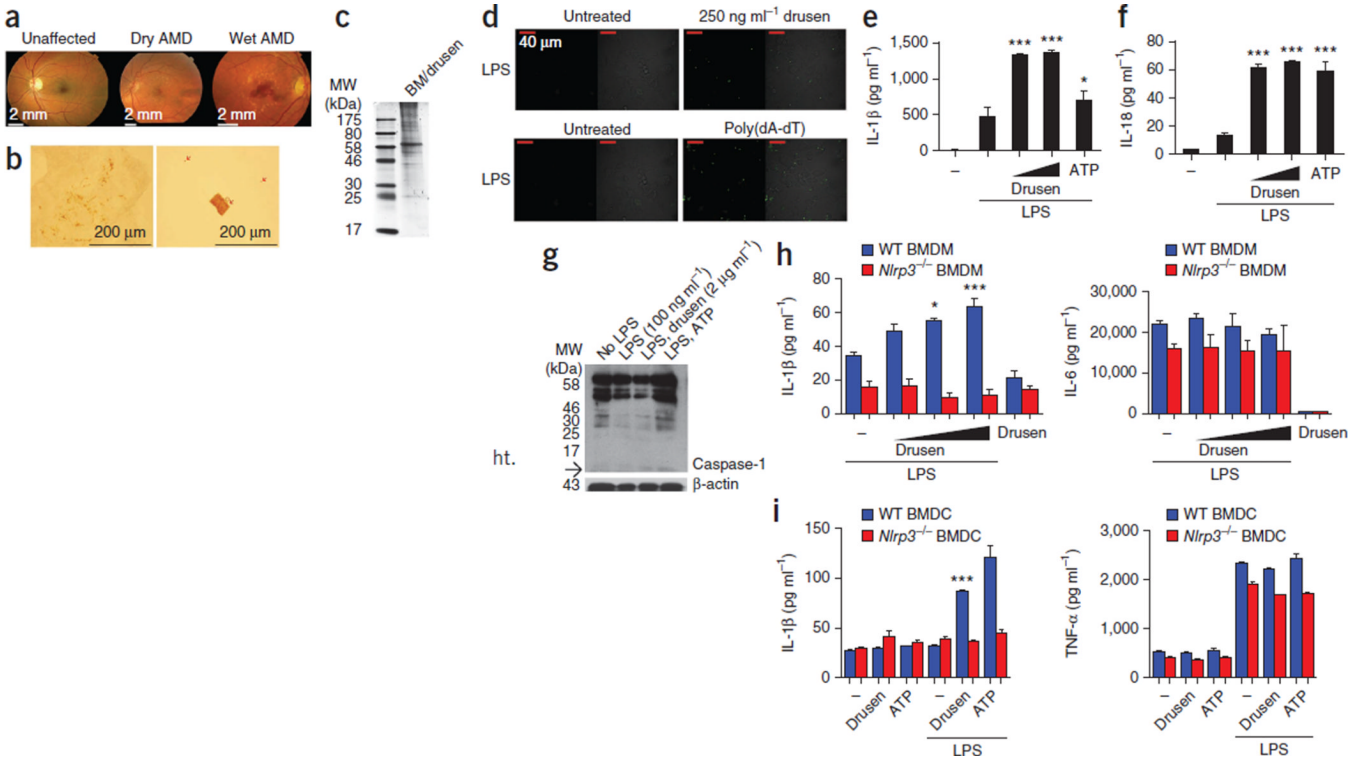


**Figure 1.**

Drusen activates the NLRP3 inflammasome. (**a**) Fundus photography from a nonsmoking unaffected individual, an individual with dry AMD and an individual with wet AMD. (**b**) Drusen fragments (arrows) in a range of sizes from just under 500 µm to submicroscopic-sized particles. (**c**) SDS-PAGE analysis of a Bruch's membrane and drusen (BM/drusen) preparation. MW, molecular weight. (**d**) Live-cell imaging of immortalized C57BL/6 BMDMs stably expressing YFP-ASC. Poly(dA-dT) was used as a positive control. Oligomerization of ASC-YFP was observed by speck formation at an original magnification of ×60. (**e**,**f**) Production of IL-1β and IL-18, as measured by ELISA in human PBMCs primed overnight with LPS and subsequently treated with increasing doses of the drusen preparation. $*P \leq 0.05$, $***P \leq 0.0001$ by analysis of variance (ANOVA) with Tukey post test compared to LPS-treated cells. (**g**) Western blot of the cleavage products of caspase-1 after treatment of THP1 cells with drusen. The arrow points to the caspase-1 p10 band. (**h**) Production of IL-1β (left) and IL-6 (right), as measured by ELISA in WT and *Nlrp3*$^{-/-}$ BMDMs after treatment with increasing doses of drusen. $*P \leq 0.05$, $***P \leq 0.0001$ by ANOVA with Tukey post test compared to LPS-treated cells. (**i**) Production of IL-1β (left) and TNF-α (right), as measured by ELISA in WT and *Nlrp3*$^{-/-}$ BMDCs after treatment with increasing doses of drusen. $***P \leq 0.0001$ by ANOVA with Tukey post test compared to LPS-treated cells. All ELISA data are representative of a minimum of three separate experiments carried out in triplicate, and all data are means ± s.e.m.

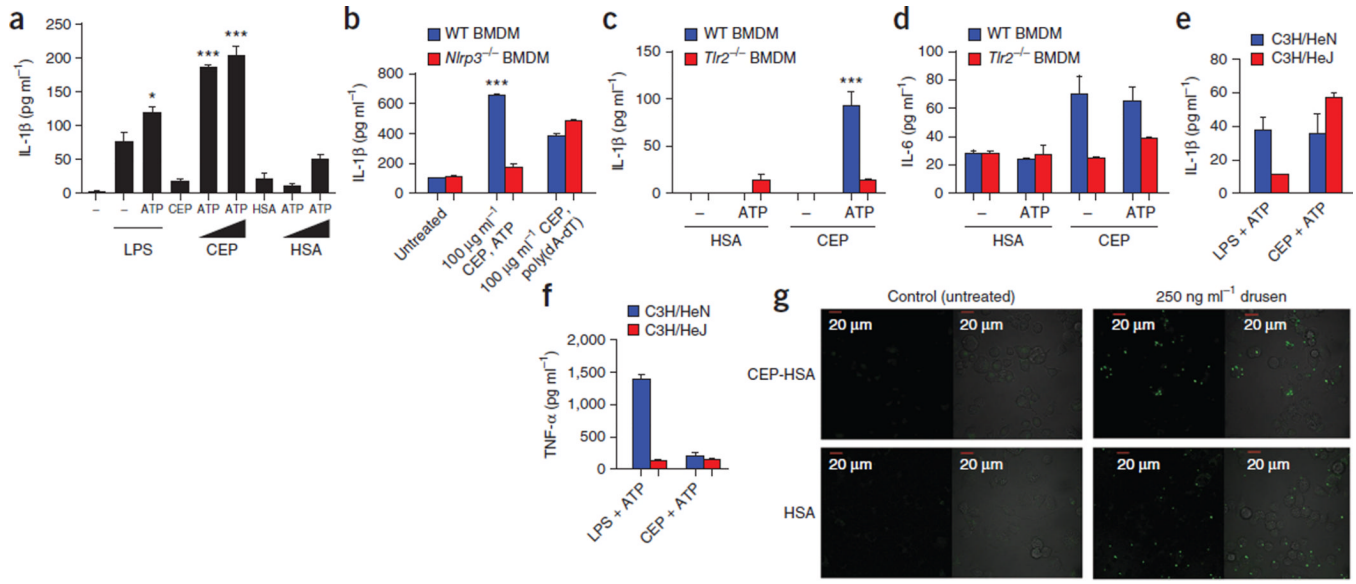


**Figure 2.**

CEP (CEP-HSA), a component of drusen, can prime the NLRP3 inflammasome. (**a**) Production of IL-1β in human PBMCs primed with LPS, CEP-HSA or HSA alone in increasing doses and subsequently treated with ATP. *$P \leq 0.05$, ***$P \leq 0.0001$ by ANOVA with Tukey post test compared to LPS-treated cells. (**b**) IL-1β production in WT and *Nlrp3*$^{-/-}$ BMDMs primed with CEP-HSA and then activated with either ATP or poly(dA-dT). ***$P \leq 0.0001$ by ANOVA with Tukey post test compared to *Nlrp3*$^{-/-}$ cells. (**c**,**d**) IL-1β and IL-6 production in WT or *Tlr2*$^{-/-}$ BMDMs primed with HSA or CEP-HSA and activated with ATP or left untreated. ***$P \leq 0.0001$ by ANOVA with Tukey post test for WT BMDMs treated with CEP-HSA and ATP compared to *TLR2*$^{-/-}$ BMDMs treated with CEP-HSA and ATP. (**e**,**f**) IL-1β and TNF-α production measured in C3H/HeN BMDMs or C3H/HeJ BMDMs primed with either LPS or CEP and activated with ATP. (**g**) Live-cell imaging of immortalized C57BL/6 BMDMs stably expressing YFP-ASC. Shown are cells primed with CEP-HSA (top) or HSA (bottom), followed by treatment with drusen. Oligomerization of ASC-YFP was observed by speck formation at an original magnification of ×60. All ELISA data are representative of a minimum of three separate experiments carried out in triplicate, and all data are means ± s.e.m.

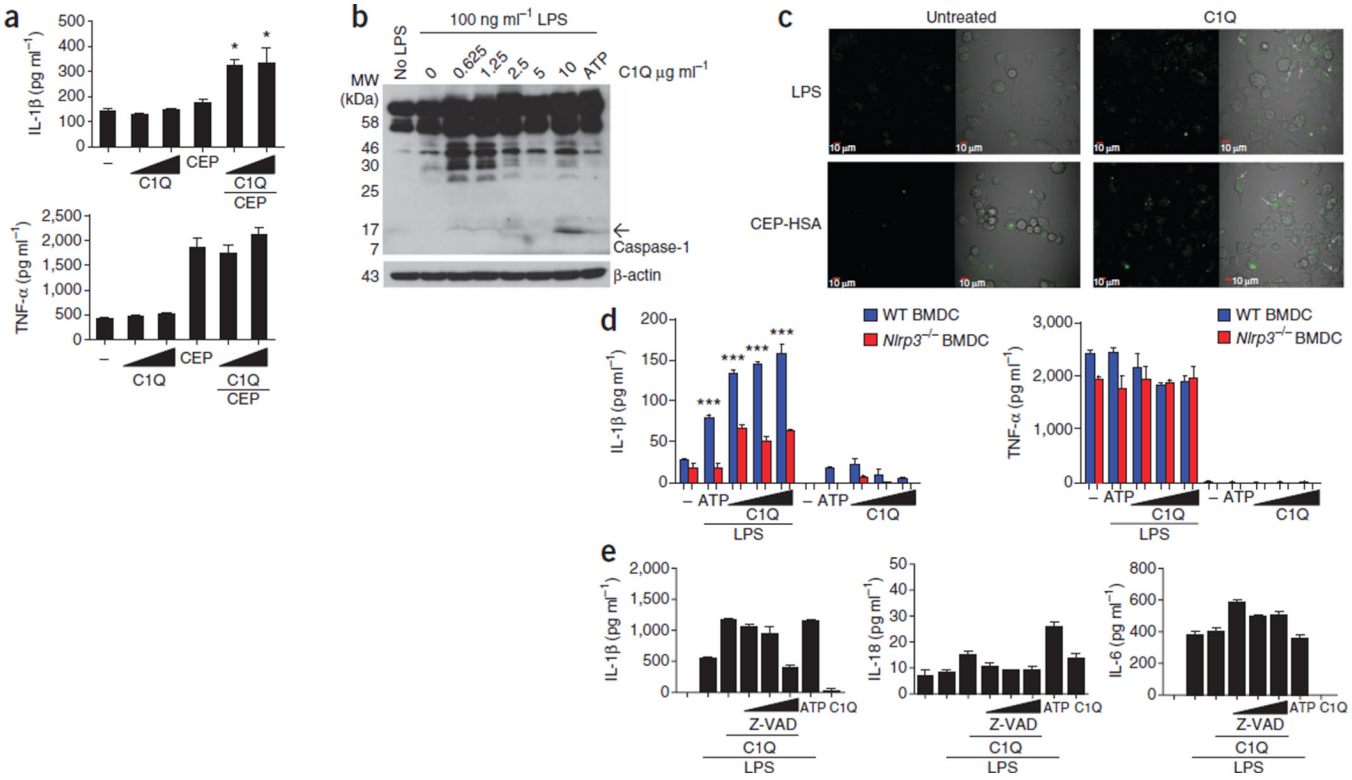


**Figure 3.**

Complement factor C1Q, a component of drusen, activates the NLRP3 inflammasome. (**a**) Production of IL-1β (top) and TNF-α (bottom) in WT BMDMs primed with CEP-HSA and activated with increasing doses of C1Q. **P* ≤ 0.05 by ANOVA with Tukey post test compared to CEP-HSA treatment alone. (**b**) Western blot of caspase-1 cleavage products in THP1 cells primed with LPS and treated with increasing doses of C1Q. The arrow points to the caspase-1 p10 band. (**c**) Live-cell imaging of immortalized C57BL/6 BMDMs stably expressing YFP-ASC. Shown are cells primed with either LPS (top) or CEP-HSA, followed by treatment with C1Q (right). Oligomerization of ASC-YFP was observed by speck formation at an original magnification of ×60. (**d**) IL-1β (left) and TNF-α (right) production in WT and *Nlrp3*$^{-/-}$ BMDCs primed with LPS and activated with increasing doses of C1Q. ****P* ≤ 0.0001 by ANOVA with Tukey post test for WT BMDCs compared to *NLRP3*$^{-/-}$ BMDCs for each given treatment. (**e**) IL-1β, IL-18 and IL-6 production in human PBMCs primed with LPS overnight and activated with C1Q, with the addition of increasing doses of Z-VAD before C1Q treatment. All ELISA data are representative of a minimum of three separate experiments carried out in triplicate, and all data are means ± s.e.m.

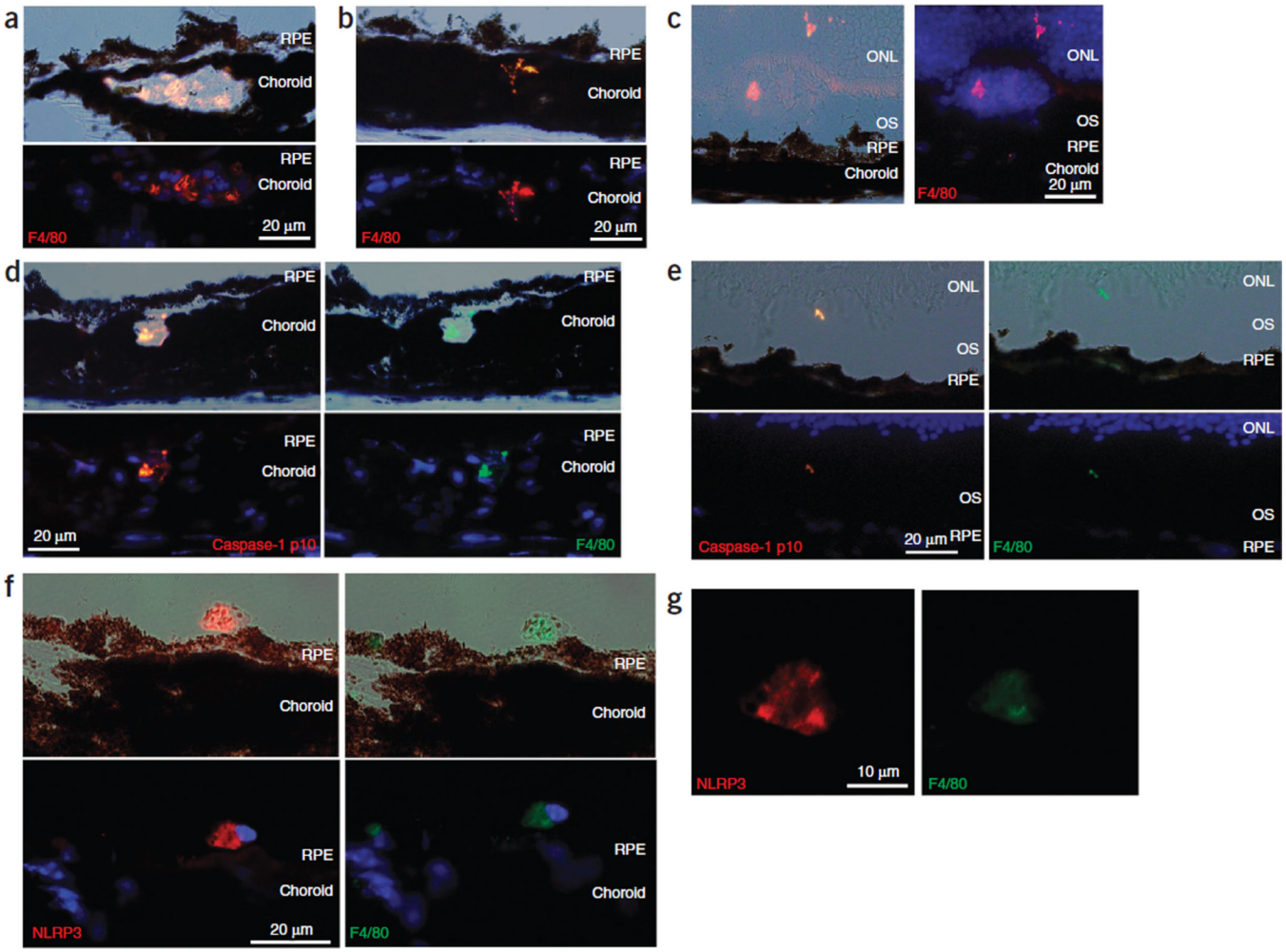


**Figure 4.**

Cleaved caspase-1 p10 colocalizes with activated macrophages in CEP-MSA–immunized mice. (**a**–**c**) Immunostaining of retinal cryosections of CEP-MSA–immunized mice showing localization of F4/80$^{+}$ macrophages to regions of the choroid (**a**), extending from the choroid toward the Bruch's membrane (**b**) and present above the RPE in the outer segments (OS) and outer nuclear layer (ONL) of the retina (**c**). Differential contrast images are shown at the top in **a** and **b** and on the left in **c**, and fluorescent images (with F4/80 in red and DAPI in blue) are shown at the bottom in **a** and **b** and on the right in **c**. (**d**,**e**) Colabeling of retinal cryosections of CEP-MSA–immunized mice, with caspase-1 p10 (red) and F4/80 (green) showing colocalization in a macrophage present within and transcending the choroid and the Bruch's membrane (**d**) and a macrophage protrusion in the outer segment of the retina (**e**). (**f**) Colabeling of retinal cryosections of CEP-MSA–immunized mice showing colocalization of NLRP3 (red) and F4/80 (green). (**g**) A higher magnification of the NLRP3 and F4/80 staining in **f**.

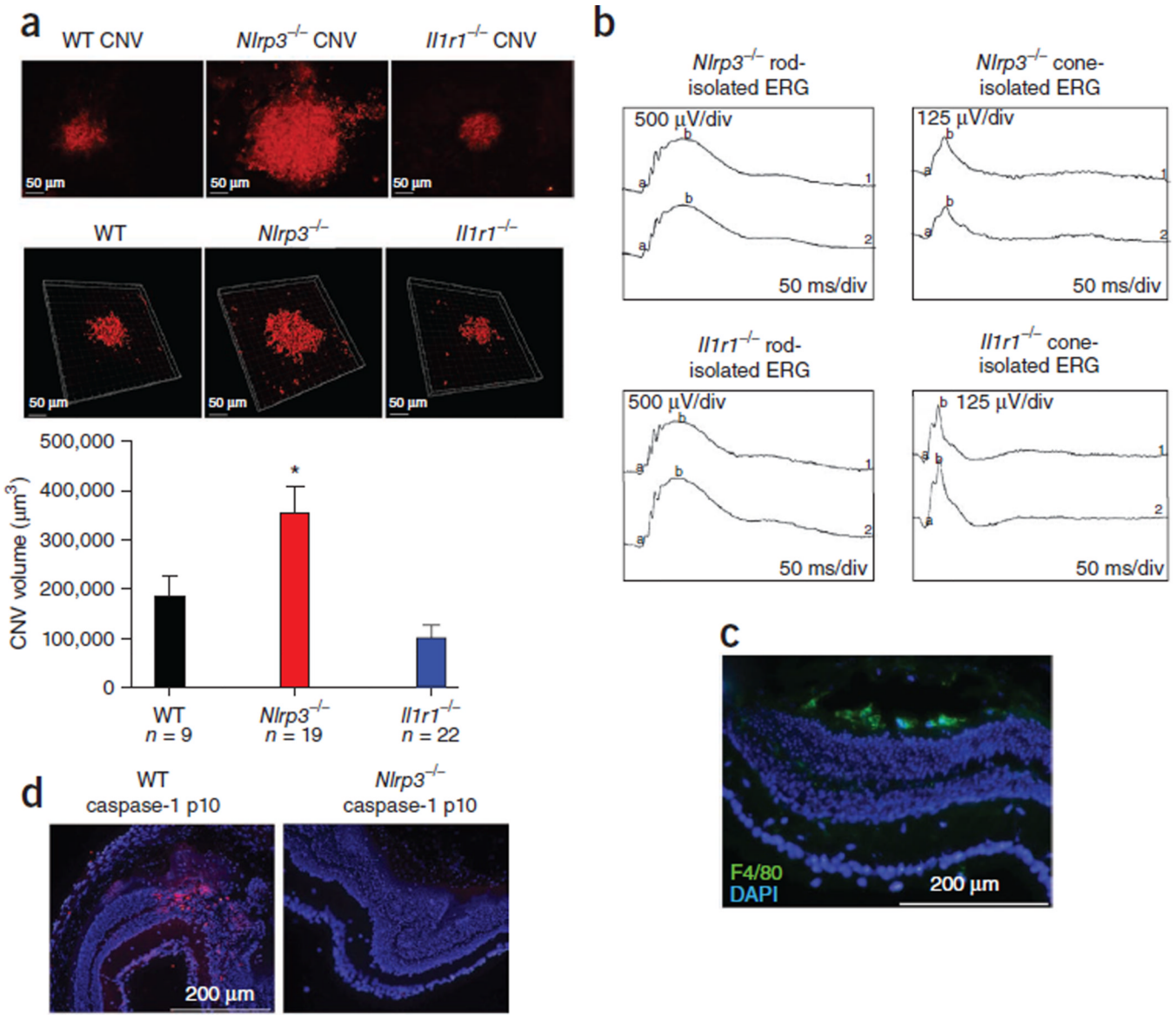


**Figure 5.**

NLRP3 is protective against laser-induced CNV lesion formation in an IL-1β–independent manner. (**a**) Laser-induced CNV in WT (top left), *Nlrp3*$^{-/-}$ (top middle) and *Il1r1*$^{-/-}$ (top right) mice showing CNV development after laser burn. Three-dimensional reconstructed images of confocal z-stacks from WT (bottom left), *Nlrp3*$^{-/-}$ (bottom middle) and *Il1r1*$^{-/-}$ (bottom right) mice. Also shown is a CNV volume rendering (bar chart). *$P \leq 0.0496$ by ANOVA followed by Tukey *post-hoc* test. Data are means ± s.e.m. (**b**) ERG analysis of rod and cone function in *Nlrp3*$^{-/-}$ and *Il1r1*$^{-/-}$ mice. The a wave represents hyperpolarization of photoreceptors, and the b wave represents the second-order neuron response. (**c**) Immunostaining showing localization of activated macrophages (F4/80, green) to the site of laser-induced injury in *Nlrp3*$^{-/-}$ mice. (**d**) Immunostaining for cleaved caspase-1 (red) of WT (left) or *Nlrp3*$^{-/-}$ (right) retinal cryosections after injury.

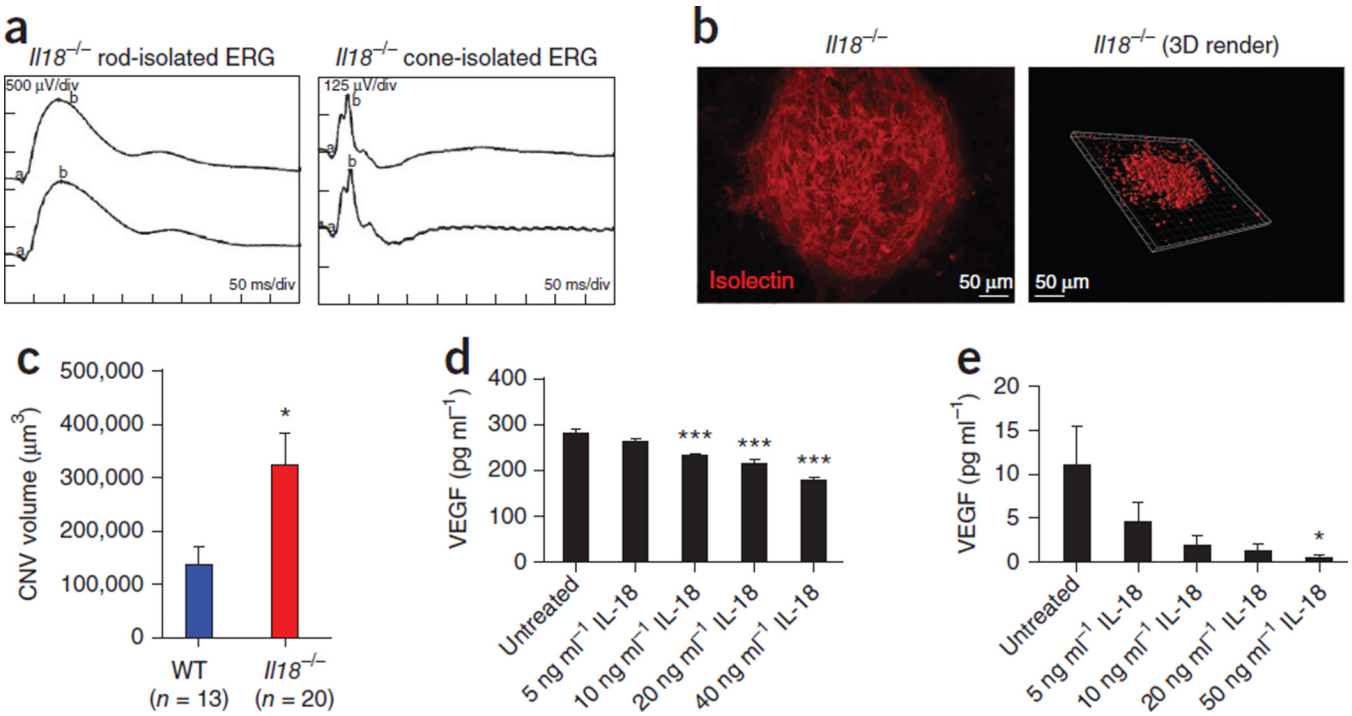


**Figure 6.**

NLRP3 confers its protection against CNV lesion formation through its role in IL-18 production, which in turn regulates VEGF concentrations. (**a**) ERG analysis of rod and cone function in *Il18*$^{-/-}$ mice. (**b**) Laser induced CNV in *Il18*$^{-/-}$ mice showing CNV development after laser burn (left). Three-dimensional (3D) reconstructed images of confocal z-stacks (right). (**c**) CNV volumes in *Il18*$^{-/-}$ and WT mice (Fig. 5). **P* = 0.0292 by Student's *t* test. (**d**,**e**) The production of VEGF, as assayed by ELISA in ARPE-19 cells (**d**) and bEnd.3 cells (**e**) treated with increasing doses of IL-18 or left untreated. **P* ≤ 0.05, ****P* ≤ 0.0001 by ANOVA with Tukey post test compared to untreated cells. ELISA data are representative of a minimum of three separate experiments carried out in triplicate, and all data are means ± s.e.m.